

Second order scheme for self-similar solutions of a time-fractional porous medium equation on the half-line

Hanna Okraśńska-Płociniczak*, Łukasz Płociniczak^{†,‡}

Abstract

Nonlocality in time is an important property of systems in which their present state depends on the history of the whole evolution. Combined with the nonlinearity of the process it poses serious difficulties in both analytical and numerical treatment.

We investigate a time-fractional porous medium equation that has proved to be important in many applications, notably in hydrology and material sciences. We show that the solution of both free boundary Dirichlet, Neumann, and Robin problems on the half-line satisfies a Volterra integral equation with non-Lipschitz nonlinearity. Based on this result we prove existence, uniqueness, and construct a family of numerical methods that solve these equations outperforming the usual naïve finite difference approach. Moreover, we prove the convergence of these methods and illustrate the theory with several numerical examples.

Keywords: numerical method, porous medium equation, anomalous diffusion, fractional derivative, Volterra equation, non-Lipschitz

AMS Classification: 35R11, 45G10, 65R20

1 Introduction

During the last few decades experimentalists, modellers, theoreticians, and numerical analysts have been investigating many aspects of nonlocality in mathematical objects. These inquiries have certainly been motivated by an increasingly rich experimental evidence for anomalous behaviour, mathematically nontrivial models, and professional curiosity. Apart from many applications, probably the one that is most researched is the so-called anomalous diffusion that arises when the transport is slower or faster than in the classical case [46, 42]. Probabilistically, this can be characterised with a deviation from the linear mean-square displacement for a randomly walking particle [41]. There is a broad experimental evidence of such dynamics in quantum optics [60], physics of plasma [21], movement of bacteria and amoeba [43], G-protein on cell surface [63], hydrology [20, 50, 51, 32, 62], and motion of dislocations in crystal lattice [37].

The nonlocality in the anomalous diffusion is usually modelled with a use of the fractional derivative [46]. There are many definitions of such operators and it depends on the situation which one is the most suited for a specific model. For example, temporal nonlocality can be described with Riemann-Liouville or Caputo derivatives while nonlocality in space requires „symmetric” operator such as the fractional Laplacian [58, 17, 18, 66, 9]. Physical derivations of the fractional porous

*Department of Mathematics, Wrocław University of Environmental and Life Sciences, ul. C.K. Norwida 25, 50-275 Wrocław, Poland

[†]Faculty of Pure and Applied Mathematics, Wrocław University of Science and Technology, Wyb. Wyspiańskiego 27, 50-370 Wrocław, Poland

[‡]Email: lukasz.plociniczak@pwr.edu.pl

media equation have been given for example in [52, 54]. We have argued there that the emergence of the time-fractional derivative is a manifestation of the waiting-time phenomenon happening in the medium, i.e. the fluid can be trapped in certain regions for prolonged periods of time which leads to the so-called subdiffusion. Recently, some experimental evidence has been given in [31] that supports this hypothesis. On the other hand, the spatial nonlocality in the porous medium equation is a consequence of the long jump phenomenon (for a physical derivation see [54]). That is to say, due to medium's complex geometry and heterogeneity fluid parcels can traverse relatively long distances in short amounts of time what in the literature is called superdiffuion. Mathematically this leads to the fractional gradient operator which is closely related to the fractional Laplacian [18, 8, 28]. A thorough summary of the theory of the fractional porous medium equation can be found [67].

Our previous studies investigated the time-fractional porous medium equation applied as a model for moisture transport in construction materials

$$\partial_t^\alpha u = (u^m u_x)_x, \quad 0 < \alpha < 1, \quad m > 1, \quad (1)$$

where the fractional derivative is of the Riemann-Liouville type

$$\partial_t^\alpha u(x, t) = \frac{1}{\Gamma(1 - \alpha)} \frac{\partial}{\partial t} \int_0^t (t - s)^{-\alpha} u(x, s) ds. \quad (2)$$

with the vanishing initial condition and dry medium at infinity

$$u(x, 0) = 0, \quad u(\infty, t) = 0, \quad x > 0, \quad t > 0. \quad (3)$$

The parameters α and m are associated with a specific experiment and are subject to fitting with the data. Based on [62] we can think that usually $\alpha \in [0.6, 1]$ while $m \approx 7 - 8$. The parameter α denotes the level of nonlocality of the model with $\alpha = 1$ being the classical case. Since, as will be seen below, our model (1) describes a slower evolution than in the classical case we speak about subdiffusion.

In previous works we have proved existence and uniqueness of a self-similar solution to the Dirichlet problem [57], provided some approximations [51], solved inverse problem of diffusivity identification [53], and constructed a numerical scheme [55]. This numerical method, although only first order accurate, provided a superior performance over the finite difference method applied to the governing PDE. The idea was to use a series of transformations leading to a nonlinear Volterra equation and then to discretize it. In this work we follow a similar route but now we introduce several improvements. First of all, we sketch how to construct an arbitrarily high order scheme and explicitly devise the second order accurate linear method. Then, we prove its convergence under some mild assumptions. The difference from our previous work is that we use the general theory of Volterra equations in order to anticipate the behaviour of its solution. This lets us to conduct yet another transformation which facilitates the crucial step in the convergence proof yielding a stronger result. Moreover, our method is constructed in a way that it gives exact results for power functions which are the leading-order approximations to the solution of the time-fractional porous medium equation. This further improves the accuracy within the second order. For example, as will be shown below, computing the wetting front to several decimal places requires using only moderate step sizes.

There is a vast literature concerning numerical methods for fractional differential equations. For general surveys one can refer to [26, 6]. The linear fractional diffusion either with temporal or spatial nonlocality has been solved for example in [64, 44, 68]. Moreover, an interesting discretizations of the fractional Laplacian have been given in [38, 19]. On the other hand, the case of nonlinear anomalous diffusion has been rigorously treated only in relatively few papers (especially when the diffusivity is a function of the solution). For example, the space-fractional porous medium has been discretized in [22] with the use of finite difference method applied to the extension problem [17]. Furthermore, in [23, 24] some very robust numerical methods have been devised, thoroughly analysed, and applied to a very broad classes of nonlocal equations. Moreover, authors of [35] used a multi-grid waveform

method for the time-fractional case. The nonlinear source terms have been considered in [7, 69]. The main difficulty in the analysis of the porous medium equation (even in the classical case) is the degeneracy of diffusivity, i.e. the coefficient of u_x can vanish. This fact makes both theoretical and numerical studies interesting and non-trivial. For several years many approaches of numerical treatment of the classical porous medium equation have been proposed. To paint the background we mention only a few papers. For example, in [25] authors used a finite difference method with an interface tracking algorithm. This feature is crucial since due to degeneracy in many circumstances the solution is characterized with a finite speed of propagation what translates into a free-boundary problem [65, 61]. Also, a finite element method for the classical porous medium equation has been analysed in [2, 29, 39]. This topic is still vigorously investigated and mathematicians constantly develop some new approaches (for ex. [33, 59, 30]).

The root of our method lies in appropriate discretization of a nonlinear Volterra equation (for a thorough treatment see [10]). A survey of numerical methods for such problems can be found in [5, 45]. Notice that the majority of the theory concerns Lipschitz nonlinearity while our model fails to satisfy this condition. There are only a few papers that developed rigorous methods for nonlipschitzian case [34]. Notably, in [11] an iterative scheme has been proposed. We also mention our previous work [56] where an idea for a proof similar to the one used in the present paper originated. Finally, in [12, 3] a highly readable theoretical summaries about non-Lipschitz problems have been published.

As we mentioned before, this paper concerns a high order numerical method for finding self-similar solutions of (1). In Section 2 we perform a series of transformations that reduce the main nonlocal nonlinear PDE into an ordinary Volterra equation with non-Lipschitz nonlinearity. As a side result we prove a existence and uniqueness result about self-similar solutions on the half-line with Dirichlet, Neumann, and Robin conditions. Next, in Section 3 we present a general scheme of numerical method construction along with explicit formulas for a second order linear interpolation scheme (trapezoidal). We also prove that it is convergent provided that the parameter m is sufficiently large. In Section 4 we illustrate our theory with numerical examples concerning some exemplary equations and the time-fractional porous medium equation itself. We close the paper with some concluding remarks.

2 Self-similar solutions and Volterra equations

In applications one is frequently interested in finding self-similar solution of (1) in the form

$$u(x, t) = t^a U(\eta), \quad \eta = xt^{-b}, \quad (4)$$

where $a, b \geq 0$ are constants to be found and the similarity variable is denoted by η . When we plug the above into the original PDE (1) we transform the spatial

$$(u^m(x, t)u_x(x, t))_x = t^{a(m+1)-2b} \frac{d}{d\eta} \left(U^m(\eta) \frac{d}{d\eta} U(\eta) \right). \quad (5)$$

and the temporal derivatives

$$\begin{aligned} \partial_t^\alpha u(x, t) &= \frac{\partial}{\partial t} (I_t^{1-\alpha} (t^a U(xt^{-b}))) = \frac{1}{\Gamma(1-\alpha)} \frac{\partial}{\partial t} \int_0^t (t-z)^{-\alpha} z^a U(xz^{-b}) dz \\ &= \frac{1}{\Gamma(1-\alpha)} \frac{\partial}{\partial t} \left(t^{a-\alpha+1} \int_0^1 (1-s)^{-\alpha} s^a U(\eta s^{-b}) ds \right), \end{aligned} \quad (6)$$

If we further introduce the Erdélyi-Kober fractional integral operator (see [40])

$$I_\delta^{\beta, \gamma} U(\eta) = \frac{1}{\Gamma(\gamma)} \int_0^1 (1-z)^{\gamma-1} z^\beta U(\eta z^{\frac{1}{\delta}}) dz, \quad (7)$$

| Condition | a | A | $b = B$ | η^* |
|----------------|----------------------|---------------------------|-------------------------|--|
| Dirichlet (11) | 0 | $1 - \alpha$ | $\frac{\alpha}{2}$ | $\frac{1}{\sqrt{y(1)^m}}$ |
| Neumann (12) | $\frac{\alpha}{m+2}$ | $1 - \frac{m+1}{m+2}$ | $\frac{m+1}{m+2}\alpha$ | $\left(\frac{m+1}{(y^{m+1})'(1)}\right)^{\frac{m}{m+2}}$ |
| Robin (13) | $\frac{\alpha}{m}$ | $1 - \frac{m-1}{m}\alpha$ | α | $\frac{m}{(y^m)'(1)}$ |

Table 1: Values of a, b in (4), $A = A(\alpha, m)$, $B = B(\alpha, m)$ as in (14), and the wetting front η^* defined in (16) for different types of boundary conditions.

we can write (1) as

$$t^{\alpha+am-2b} \frac{d}{d\eta} \left(U^m \frac{dU}{d\eta} \right) = \left[(1 - \alpha + a) - b\eta \frac{d}{d\eta} \right] I_{-\frac{1}{b}}^{a, 1-\alpha} U, \quad 0 < \alpha < 1, \quad (8)$$

Now, the self-similar solution is possible only if

$$2b - ma = \alpha, \quad (9)$$

which is the consistency condition. Since there are two unknowns: $a = a(\alpha, m)$ and $b = b(\alpha, m)$ we need yet another equation. This comes from the initial-boundary conditions and we assume that initially the medium is dry (3) which expressed in the self-similar variables (4) yields

$$U(\infty) = 0. \quad (10)$$

Furthermore, for the boundary conditions we have several self-similar physically relevant choices. For example, we can consider the Dirichlet

$$u(0, t) = 1, \quad x > 0, \quad (11)$$

which describes constant concentration, Neumann

$$u^m(0, t)u_x(0, t) = -1, \quad x > 0, \quad (12)$$

describing constant flux, or Robin problem

$$u^m(0, t)u_x(0, t) = -u(0, t), \quad x > 0, \quad (13)$$

which translates into requirement that the flux is proportional to the concentration at the interface $x = 0$. For a physical account of these models see [52]. Boundary conditions provide us with the second equation for a and b and eventually we are able to write (1) as

$$\frac{d}{d\eta} \left(U^m \frac{dU}{d\eta} \right) = AI_{-\frac{1}{b}}^{a, 1-\alpha} U - B\eta \frac{d}{d\eta} I_{-\frac{1}{b}}^{a, 1-\alpha} U, \quad 0 < \alpha < 1, \quad (14)$$

for some $A = A(\alpha, m)$ and $B = B(\alpha, m)$. The exact values of these constants for different boundary conditions are summarized in Tab. 1. Note that always $A, B \geq 0$.

To motivate our further reasoning let us focus on the Robin problem (13) for which

$$a = \frac{\alpha}{m}, \quad b = \alpha. \quad (15)$$

Other conditions have been considered in [52, 57] and lead to a similar final integral equation. In any of the considered boundary conditions the support of the solution will be compact (for a proof see [27] and for the classical case [4]). Physically, this fact is equivalent to a finite speed of wetting front propagation and arises in the degeneracy of the equation (1). Having that in mind, let $\eta > 0$ be such that

$$U(\eta) = 0 \quad \text{for} \quad \eta > \eta^*. \quad (16)$$

Moreover, by integrating (14) one can show that there is no flux through the support's boundary (see [57])

$$U(\eta)^m \frac{dU}{d\eta}(\eta) = 0 \quad \text{for} \quad \eta > \eta^*. \quad (17)$$

Note that η^* is a-priori unknown and has to be determined as a part of the solution since we are dealing with a free-boundary problem. A standard way of proceeding is to introduce yet another transformation

$$U(\eta) = Cy(z), \quad z = 1 - \frac{\eta}{\eta^*}, \quad z \geq 0, \quad (18)$$

where C has to be determined. The conditions (16)-(17) now become

$$y(0) = 0, \quad y^m(0)y'(0) = 0, \quad (19)$$

where prime denotes the differentiation with respect to z . The Robin condition (13) now yields

$$U^m(0) \frac{dU}{d\eta}(0) = -U(0) \rightarrow (y^m)'(1) = \frac{m\eta^*}{C^m}, \quad (20)$$

which gives us one equation to determine η^* and C .

When we plug (18) into (14) we obtain

$$\frac{C^m}{(\eta^*)^2} (y^m y')' = AG_\alpha y + B(1-z)(G_\alpha y)', \quad (21)$$

where for a and b as in (15) we have defined

$$\begin{aligned} G_\alpha y(z) &= \frac{1}{\Gamma(1-\alpha)} \int_{(1-z)^{1/b}}^1 (1-s)^{-\alpha} s^a y(1-s^{-b}(1-z)) ds \\ &= \frac{1}{b} \frac{1}{\Gamma(1-\alpha)} (1-z)^{\frac{a+1}{b}} \int_0^z \left(1 - \left(\frac{1-z}{1-w} \right)^{\frac{1}{b}} \right)^{-\alpha} \frac{y(w)}{(1-w)^{1+\frac{a+1}{b}}} dw. \end{aligned} \quad (22)$$

The second equality above follows from the change of variables $w = 1 - s^{-a}(1-z)$. We can thus see that

$$C = (\eta^*)^{\frac{2}{m}}, \quad (23)$$

which together with (20) closes the system and gives us an equation for η^* provided we know the solution y , that is η^* can be found from

$$\eta^* = \frac{m}{(y^m)'(1)}. \quad (24)$$

Now, (21) can be transformed into a nonlinear integral Volterra equation. First, with an integration and using the condition (19) we obtain

$$\begin{aligned} y(z)^m y'(z) &= A \int_0^z G_\alpha y(s) ds + B \int_0^z (1-z)(G_\alpha y(s))' ds \\ &= B(1-z)G_\alpha y(z) + (A+B) \int_0^z G_\alpha y(s) ds, \end{aligned} \quad (25)$$

where we have integrated by parts. A second integration finally yields

$$\begin{aligned} y(z)^{m+1} &= (m+1) \int_0^z (B(1-s) + (A+B)(z-s)) G_\alpha y(s) ds \\ &=: \int_0^z F(z, s) G_\alpha y(s) ds. \end{aligned} \quad (26)$$

Next, we use the definition of G_α operator (22) and change the order of integration (Fubini's theorem)

$$y(z)^{m+1} = \frac{1}{b} \frac{1}{\Gamma(1-\alpha)} \int_0^z \left(\int_u^z F(z, s) (1-s)^{\frac{a+1}{b}} \left(1 - \left(\frac{1-s}{1-u} \right)^{\frac{1}{b}} \right)^{-\alpha} ds \right) \frac{y(u) du}{(1-u)^{1+\frac{a+1}{b}}}. \quad (27)$$

We can now substitute back $v = ((1-s)/(1-u))^{1/b}$ inside the inner integral to obtain

$$\begin{aligned} y(z)^{m+1} &= \frac{1}{\Gamma(1-\alpha)} \int_0^z \left[\int_{(\frac{1-z}{1-u})^{1/b}}^1 F(z, 1-s^b(1-u)) (1-s)^{-\alpha} s^a ds \right] y(u) du \\ &=: \int_0^z K(z, u) y(u) du, \end{aligned} \quad (28)$$

where we have defined the kernel K . Observe that it can be written as a combination of incomplete beta functions (and we use this fact later). Moreover, the kernel is a continuous function since $(1-s)^{-\alpha}$ is integrable near $s=1$ and $a > 0$. We can also obtain some simple bounds on K due to the fact that $F(z, s)$ is a linear function in its both variables. Assume that $0 \leq z \leq X$ for some $0 < X < 1$. Then,

$$B(1-X) \leq F(z, s) \leq A+2B, \quad (29)$$

and hence

$$K(z, u) \leq \frac{m+1}{\Gamma(1-\alpha)} (A+2B) \int_{(\frac{1-z}{1-u})^{1/b}}^1 (1-s)^{-\alpha} ds = \frac{m+1}{\Gamma(2-\alpha)} (A+2B) \left(1 - \left(\frac{1-z}{1-u} \right)^{1/b} \right)^{1-\alpha}. \quad (30)$$

Now, we have

$$\frac{1-z}{1-s} = 1 - \frac{z-s}{1-s}, \quad (31)$$

what together with elementary estimate $(1-x)^\gamma \geq 1 - \gamma x$ for $\gamma \geq 1$ leads to

$$K(z, u) \leq \frac{m+1}{\Gamma(2-\alpha)} (A+2B) \left(\frac{1}{b} \frac{z-u}{1-X} \right)^{1-\alpha} \leq K_+(z-u)^{1-\alpha}, \quad (32)$$

because $0 \leq u \leq z \leq X$. Similarly, we can obtain bounds from below. To this end, notice that

$$\begin{aligned} K(z, u) &\geq \frac{m+1}{\Gamma(1-\alpha)} B(1-X) \left(\frac{1-z}{1-u} \right)^{a/b} \int_{(\frac{1-z}{1-u})^{1/b}}^1 (1-s)^{-\alpha} ds \\ &= \frac{m+1}{\Gamma(2-\alpha)} B(1-X) \left(\frac{1-z}{1-u} \right)^{a/b} \left(1 - \left(\frac{1-z}{1-u} \right)^{1/b} \right)^{1-\alpha}. \end{aligned} \quad (33)$$

Using the convexity bound $(1-x)^\gamma \leq 1 - \gamma x$ for $\gamma \geq 1$ we now have

$$K(z, u) \geq \frac{m+1}{\Gamma(2-\alpha)} B(1-X) \left(\frac{1-z}{1-u} \right)^{a/b} \left(\frac{z-u}{1-u} \right)^{1-\alpha} \geq K_-(z-u)^{1-\alpha}, \quad (34)$$

since $0 \leq u \leq z \leq X$. Whence, we have found the behaviour of the kernel yielding

$$K_-(z-u)^{1-\alpha} \leq K(z,u) \leq K_+(z-u)^{1-\alpha}, \quad (35)$$

where K_{\pm} are known constants. These kernel bounds have important consequence for the form of the solution and are crucial for our subsequent construction of the numerical method. For example, as was shown in [13] (for a further account see also [36, 14, 16, 15, 48]) the equation (28) has a unique non-trivial solution which satisfies

$$C_-^{\frac{1}{m}} z^{\frac{2-\alpha}{m}} \leq y(z) \leq C_+^{\frac{1}{m}} z^{\frac{2-\alpha}{m}}, \quad (36)$$

where $C_{\pm} > 0$ can be found explicitly, however, their exact values are not relevant for our reasoning. The calculations for other boundary conditions presented in Tab. 1 are essentially identical. Therefore, we have shown the following result.

Theorem 1. *Let $u = u(x, t)$ satisfy (1) with vanishing initial condition and along with one of the self-similar boundary conditions (11)-(13). Then,*

$$u(x, t) = (\eta^*)^{\frac{2}{m}} t^a y \left(1 - \frac{1}{\eta^*} \frac{x}{t^b} \right), \quad (37)$$

where $y = y(z)$ is a unique nontrivial solution of the Volterra equation (28) while a , b , and η^* are given in Tab. 1. Moreover, u satisfies the following estimates

$$U_- \left(1 - \frac{1}{\eta^*} \frac{x}{t^b} \right)^{\frac{2-\alpha}{m}} \leq u(x, t) \leq U_+ \left(1 - \frac{1}{\eta^*} \frac{x}{t^b} \right)^{\frac{2-\alpha}{m}}, \quad (38)$$

with suitable constants $U_{\pm} > 0$ that can be found explicitly.

3 Numerical method

In the previous section we have shown that looking for solutions of (1) with self-similar boundary conditions (11)-(13) is equivalent to solving (28). Therefore, in what follows we will devise a numerical method for solving a general class of nonlinear Volterra equations of the form

$$y(z)^{m+1} = \int_0^z K(z, s) y(s) ds, \quad 0 \leq z \leq 1, \quad (39)$$

where we assume that the kernel is continuous and there exist constants K_{\pm} such that

$$K_-(z-s)^{\gamma} \leq K(z, s) \leq K_+(z-s)^{\gamma}, \quad \gamma \geq 0. \quad (40)$$

Note that in this section we use the same letters for y and K as before, however now we are considering a *general* Volterra equation which does not have to have anything in common with anomalous diffusion. By results from [13] the above equation has a unique non-trivial solution satisfying

$$C_-^{\frac{1}{m}} z^{\frac{\gamma+1}{m}} \leq y(z) \leq C_+^{\frac{1}{m}} z^{\frac{\gamma+1}{m}}, \quad (41)$$

for suitable constants $C_{\pm} > 0$. Therefore, the behaviour of the solution is of power type and for a numerical treatment it is reasonable to peel it off from the actual form of y . That is to say, we substitute

$$y(z) = z^{\frac{\gamma+1}{m}} v(z), \quad (42)$$

which leads to an equivalent integral equation

$$v(z) = z^{-\frac{(m+1)(\gamma+1)}{m}} \int_0^z K(z, s) s^{\frac{\gamma+1}{m}} v(s) ds. \quad (43)$$

It is crucial to note that v is now bounded away from zero, that is

$$0 < C_-^{\frac{1}{m}} \leq v(z) \leq C_+^{\frac{1}{m}}, \quad (44)$$

what facilitates both the analysis and numerical computations. A particular choice of the kernel, i.e. when $K(z, s) = K_+(z - s)^\gamma$ clearly leads to a constant solution

$$v(z) = \left(K_+ \beta \left(\gamma + 1, \frac{\gamma + 1}{m} + 1 \right) \right)^{\frac{1}{m}}, \quad (45)$$

where β is Euler beta function. This simple solution can serve as a benchmark of various numerical methods.

3.1 Construction

Now we can proceed to the discretization. Introduce the grid

$$z_n := \frac{n}{N}, \quad h := \frac{1}{N}, \quad n = 0, 1, \dots, N, \quad (46)$$

where the total number of grid points N is fixed. Further, we can discretize the integral in (43)

$$\int_0^{z_n} K(z_n, s) s^{\frac{\gamma+1}{m}} v(s) ds = \sum_{i=0}^{n-1} (w_{n,i}(h) v(z_i) + \delta_i(h)), \quad (47)$$

where $\delta_i(h)$ is the local consistency error, and $w_{n,i}(h)$ are weights that depend on the form of the kernel. When we use (47) in (43) and truncate the remainder we obtain the following numerical scheme

$$v_n^{m+1} = z_n^{-\frac{(m+1)(\gamma+1)}{m}} \sum_{i=0}^{n-1} w_{n,i}(h) v_i, \quad (48)$$

where by v_i we have denoted the numerical approximation to $v(z_i)$ while $K_{n,i} = K(z_n, z_i)$. Note also that in the quadrature (47) we have not included the last point of the interval $[0, z_n]$. This leads to a (half-)open quadrature and has been chosen in order to reduce the computational cost of the method. For if the sum on the right-hand side of the above included v_n term we would obtain an implicit method that would require solving a nonlinear equation of the form $x^{m+1} - a_1 x + a_0 = 0$ in each step. In order to keep the cost as low as possible and to improve accuracy we consider only explicit methods.

Different quadratures would yield different values of the weights $w_{n,i}(h)$. For example, the simplest rectangular rule in which the whole integrand is approximated by its value at the lower terminal would yield

$$w_{n,i}(h) = h K(z_n, z_i) z_i^{\frac{\gamma+1}{m}}. \quad (49)$$

This method could be proved to be convergent (see [55]), however, it does not solve the constant case exactly, that is to say when $K(z, s) = K_+(z - s)^\gamma$ the numerical solution v_n is not equal to (45). To see this suppose that $v_0 = v_1 = v_2 = C$, then from (48) at $n = 2$ and (49)

$$C^{m+1} = C K_+ h^{-\frac{(m+1)(\gamma+1)}{m}+1} (2h - h)^\gamma h^{\frac{\gamma+1}{m}} = C K_+, \quad (50)$$

hence $C = (K_+)^{1/m}$. Then, the third step yields

$$v_3^{m+1} = K_+ h^{-\frac{(m+1)(\gamma+1)}{m}+1} \left((3h-h)^\gamma h^{\frac{\gamma+1}{m}} + (3h-2h)^\gamma (2h)^{\frac{\gamma+1}{m}} \right) = K_+ (2^\gamma + 1) \neq C^{m+1}, \quad (51)$$

for $\gamma > 0$. Therefore, v_n cannot be constant for all $n \geq 3$. An ability of a numerical scheme to be able to solve for a constant solution can be thought as a necessary requirement that we have to make since it would accurately resolve the zero order Taylor series term. A family of such methods can be devised by using an interpolating polynomial for the unknown v_n in the integral (47). The kernel, since it is known, is not approximated. Although in this work we will focus only on the first degree interpolation, i.e. a linear reconstruction, it is instructive to see how does the zeroth order approximation look like. To this end we write

$$\int_0^{z_n} K(z_n, s) s^{\frac{\gamma+1}{m}} v(s) ds = \sum_{i=0}^{n-1} \int_{z_i}^{z_{i+1}} K(z_n, s) s^{\frac{\gamma+1}{m}} v(s) ds, \quad (52)$$

in which we expand v in its Taylor series $v(s) = v(z_i) + v'(\xi_i)(s - z_i)$, which leads to

$$\int_0^{z_n} K(z_n, s) s^{\frac{\gamma+1}{m}} v(s) ds = \sum_{i=0}^{n-1} \left[\left(\int_{z_i}^{z_{i+1}} K(z_n, s) s^{\frac{\gamma+1}{m}} ds \right) v_i + \delta_i(h) \right], \quad (53)$$

where by the mean value theorem the remainder is

$$\delta_i(h) = v'(\xi_i) \int_{z_i}^{z_{i+1}} K(z_n, s) s^{\frac{\gamma+1}{m}} (s - z_i) ds. \quad (54)$$

Therefore, going back to (43) gives

$$v(z_n)^{m+1} = z_n^{-\frac{(m+1)(\gamma+1)}{m}} \sum_{i=0}^{n-1} \left(\int_{z_i}^{z_{i+1}} K(z_n, s) s^{\frac{\gamma+1}{m}} ds \right) v_i + \delta_n(h), \quad (55)$$

where the remainder satisfies

$$\begin{aligned} |\delta_n(h)| &\leq z_n^{-\frac{(m+1)(\gamma+1)}{m}} \sum_{i=0}^{n-1} |\delta_i(h)| = z_n^{-\frac{(m+1)(\gamma+1)}{m}} |v'(\xi)| \sum_{i=0}^{n-1} \int_{z_i}^{z_{i+1}} K(z_n, s) s^{\frac{\gamma+1}{m}} (s - z_i) ds \\ &\leq z_n^{-\frac{(m+1)(\gamma+1)}{m}} K_+ |v'(\xi)| h \sum_{i=0}^{n-1} \int_{z_i}^{z_{i+1}} (z_n - s)^\gamma s^{\frac{\gamma+1}{m}} ds. \end{aligned} \quad (56)$$

where, once again, we have used the mean value theorem and used (35). Further, with a substitution $s = nh\sigma$ we can evaluate the integral

$$|\delta_n(h)| \leq K_+ \|v'(\xi)\| \beta \left(\gamma + 1, \frac{\gamma + 1}{m} \right) h = O(h), \quad h \rightarrow 0^+, \quad (57)$$

uniformly for $n \in \mathbb{N}$. Whence, the truncation error of the method is of the first order. Here, $\beta(\cdot, \cdot)$ is the Euler beta function. Neglecting the remainder we obtain a rectangle method for solving (43)

$$v_n^{m+1} = z_n^{-\frac{(m+1)(\gamma+1)}{m}} \sum_{i=0}^{n-1} \left(\int_{z_i}^{z_{i+1}} K(z_n, s) s^{\frac{\gamma+1}{m}} ds \right) v_i. \quad (58)$$

In contrast with (49) the above method solves for the constant solution exactly by the very construction (in that case $v' \equiv 0$ and the remainder vanishes).

It is now a straightforward exercise to develop higher order methods with the use of the higher degree of Lagrange's interpolating polynomial. We will analyse only the second order method since we are able to equip it with a suitable choice of initial conditions. As we shall see below, for higher order methods a prescription of starting values is not a straightforward task. This situation is similar to multistep methods for ODEs. Having that in mind we can use a linear approximation to v in the integral in (47). The important point is to construct an explicit method by not including the terminal point of the interval into the interpolation. That is to say, we have to partition the interval $[0, z_n]$ into subintervals which contain exactly three nodes. Then, we construct a linear interpolation based on first two nodes. Due to this construction we have to consider separately cases when n is even or odd.

First, suppose that n is even. Then, we build linear approximations based on the first and second points of a three node interval starting with $z = 0$. That is to say, we have the partition

$$\int_0^{z_n} K(z_n, s) s^{\frac{\gamma+1}{m}} v(s) ds = \sum_{i=0}^{\frac{n}{2}-1} \int_{z_{2i}}^{z_{2i+2}} K(z_n, s) s^{\frac{\gamma+1}{m}} v(s) ds, \quad (59)$$

in which we use Lagrange's interpolation

$$v(s) = \left(1 - \frac{s - z_{2i}}{h}\right) v(z_{2i}) + \frac{s - z_{2i}}{h} v(z_{2i+1}) + \frac{1}{2} v''(\hat{\xi}_i) (s - z_{2i})(s - z_{2i+1}). \quad (60)$$

Here, $\hat{\xi}_i$ is the intermediate point needed in the remainder. If we use that in the integral we obtain

$$\begin{aligned} \int_0^{z_n} K(z_n, s) s^{\frac{\gamma+1}{m}} v(s) ds &= \sum_{i=0}^{\frac{n}{2}-1} w_{n,2i}(h) v(z_{2i}) + w_{n,2i+1}(h) v(z_{2i}) \\ &+ \frac{1}{2} v''(\xi) \sum_{i=0}^{\frac{n}{2}-1} \int_{z_{2i}}^{z_{2i+2}} K(z_n, s) s^{\frac{\gamma+1}{m}} (s - z_{2i})(s - z_{2i+1}) ds, \end{aligned} \quad (61)$$

where we have utilized the mean value theorems for integrals and sums. The weights are given by

$$w_{n,i}(h) = \int_{z_i}^{z_{i+2}} K(z_n, s) s^{\frac{\gamma+1}{m}} \left(\begin{cases} 1 - \frac{s - z_i}{h}, & i \text{ even} \\ \frac{s - z_i}{h}, & i \text{ odd} \end{cases} \right) ds \quad \text{for } n \text{ even and } 0 \leq i \leq n - 2. \quad (62)$$

A similar calculation can be conducted for odd values of n . In that case, however, we first linearly interpolate between z_0 and z_1 and then partition the rest of the interval $[z_1, z_n]$ into three node subintervals. We then have

$$\int_0^{z_n} K(z_n, s) s^{\frac{\gamma+1}{m}} v(s) ds = \int_0^{z_1} K(z_n, s) s^{\frac{\gamma+1}{m}} v(s) ds + \sum_{i=1}^{\frac{n-1}{2}} \int_{z_{2i-1}}^{z_{2i+1}} K(z_n, s) s^{\frac{\gamma+1}{m}} v(s) ds. \quad (63)$$

Further, conducting analogous interpolation as in the even case leads to

$$\begin{aligned} \int_0^{z_n} K(z_n, s) s^{\frac{\gamma+1}{m}} v(s) ds &= w_{n,0}(h) v(0) + \sum_{i=1}^{\frac{n-1}{2}} w_{n,2i-1}(h) v(z_{2i-1}) + w_{n,2i}(h) v(z_{2i}) \\ &+ \frac{1}{2} v''(\xi_1) \int_0^{z_1} K(z_n, s) s^{1+\frac{\gamma+1}{m}} (s - z_1) ds + \sum_{i=1}^{\frac{n-1}{2}} \int_{z_{2i-1}}^{z_{2i+1}} K(z_n, s) s^{\frac{\gamma+1}{m}} (s - z_{2i-1})(s - z_{2i}) v''(\xi_i(s)) ds, \end{aligned} \quad (64)$$

where ξ_s is an intermediate point. In that case, the weights are given by

$$\begin{aligned} w_{n,0}(h) &= \int_0^{z_1} K(z_n, s) s^{\frac{\gamma+1}{m}} \left(1 - \frac{s}{h}\right) ds, \\ w_{n,1}(h) &= \int_0^{z_1} K(z_n, s) s^{\frac{\gamma+1}{m}} \frac{s}{h} ds + \int_{z_1}^{z_3} K(z_n, s) s^{\frac{\gamma+1}{m}} \left(1 - \frac{s - z_1}{h}\right) ds, \\ w_{n,i}(h) &= \int_{z_{i-1}}^{z_{i+1}} K(z_n, s) s^{\frac{\gamma+1}{m}} \left(\begin{cases} \frac{s - z_{i-1}}{h}, & i \text{ even} \\ 1 - \frac{s - z_{i-1}}{h}, & i \text{ odd} \end{cases} \right) ds \quad \text{for } n \text{ odd and } 1 < i \leq n-1. \end{aligned} \quad (65)$$

Therefore, the whole equation (43) using our linear reconstruction can be written as

$$v(z_n)^{m+1} = z_n^{-\frac{(m+1)(\gamma+1)}{m}} \sum_{i=0}^{n-1} w_{n,i}(h) v(z_i) + \delta_n(h), \quad (66)$$

where the remainder can be estimated with the help of (61) and (64) to be

$$|\delta_n(h)| \leq K_+ \|v''\| B \left(\gamma + 1, \frac{\gamma + 1}{m} \right) h^2 =: Ch^2 = O(h^2) \quad \text{as } h \rightarrow 0^+, \quad (67)$$

uniformly for $n \in \mathbb{N}$. Therefore, by truncating the remainder we obtain a consistent second order method in the form (48) where weights are defined in (62) and (65).

Having designed a method we can move to the important question about the initial conditions for v . Since (39) always possesses a trivial solution $y \equiv 0$ we have to choose an appropriate starting value for our numerical method in order to converge to a non-trivial one. One way of doing that is to approximate the integral in (43) over the interval $z \in [0, h]$ with some simple quadrature. For example, we can use the rectangle rule in which we take the value of v at the *right* endpoint. That is, we reconstruct v with a constant function

$$v(s) = v(h) - v'(\xi_h)(h - s), \quad s \in (0, h), \quad (68)$$

for some $\xi_h \in (0, h)$. Then, from (43) we can write

$$v(h)^{m+1} = h^{-\frac{(m+1)(\gamma+1)}{m}} v(h) \int_0^h K(h, s) s^{\frac{\gamma+1}{m}} ds + R(h), \quad (69)$$

where by the mean value theorem the remainder satisfies

$$|R(h)| = h^{-\frac{(m+1)(\gamma+1)}{m}} |v'(\widehat{\xi}_h)| \int_0^h K(h, s) (h - s) s^{\frac{\gamma+1}{m}} ds \leq K_+ |v'(\widehat{\xi}_h)| B \left(\gamma + 2, \frac{\gamma + 1}{m} + 1 \right) h, \quad (70)$$

where we have used the assumption of kernel boundedness (35). Therefore, after substitution $s = z\sigma$ in (69) we have

$$v(h)^{m+1} - v(h) h^{-\gamma} \int_0^1 K(h, h\sigma) \sigma^{\frac{\gamma+1}{m}} ds = R(h). \quad (71)$$

Now, the left-hand side of the above is bounded from (35) while the right-hand side vanishes to zero when $h \rightarrow 0^+$. We can then propose that the starting step for the numerical method is

$$v_0 = v(0) = \lim_{h \rightarrow 0^+} \left(h^{-\gamma} \int_0^1 K(h, h\sigma) \sigma^{\frac{\gamma+1}{m}} ds \right)^{\frac{1}{m}}, \quad (72)$$

provided the above limit exists. We thus assume that it is the case since otherwise, the solution could be unnecessarily difficult or even meaningless to solve numerically. Note that, taking the above as an initial step in the scheme does not introduce any error apart from numerical rounding.

The initial step (72) is sufficient to start the rectangle scheme (58) however, in order to initialize the second order trapezoidal method we need a guess on the value of $v(h)$. A straightforward idea is to once again use the linear interpolation between $v(0)$ and $v(h)$ similarly as in the odd case of method's construction. But in present case it yields $v(h)$ implicitly

$$\begin{aligned} v(h)^{m+1} &= h^{-\frac{(m+1)(\gamma+1)}{m}} \int_0^h K(h, s) s^{\frac{\gamma+1}{m}} v(s) ds \\ &= h^{-\frac{(m+1)(\gamma+1)}{m}} \left[v(0) \int_0^h K(h, s) s^{\frac{\gamma+1}{m}} \left(1 - \frac{s}{h}\right) ds + v(h) \int_0^h K(h, s) s^{\frac{\gamma+1}{m}} \frac{s}{h} ds \right] + R(h), \end{aligned} \quad (73)$$

where, similarly as before, the remainder is $R(h) = O(h^2)$ as $h \rightarrow 0^+$. After truncation, the second initial condition v_1 can be found by solving the nonlinear equation

$$h^{\frac{(m+1)(\gamma+1)}{m}} v_1^{m+1} - \left(\int_0^h K(h, s) s^{\frac{\gamma+1}{m}} \frac{s}{h} ds \right) v_1 - \left(\int_0^h K(h, s) s^{\frac{\gamma+1}{m}} \left(1 - \frac{s}{h}\right) ds \right) v_0 = 0. \quad (74)$$

Observe that solving the above is required only once at the initialization phase of the second order method. Therefore, (72) and (74) supply us with at worst a second order approximation of the starting values for the scheme (48) along with weights (62) and (65).

3.2 Convergence

Before we proceed to the convergence proof of (48) with weights (62) and (65) we present two auxiliary results that will be used later. The first one is a variation on a discrete version of the classical Grönwall-Bellman's lemma.

Lemma 1. *Let $\{e_n\}$, $n = 1, 2, \dots$ be a sequence of positive numbers satisfying*

$$e_n \leq \frac{\mu}{n} \sum_{i=1}^{n-1} e_i + \delta, \quad n \geq 1, \quad (75)$$

where $\mu, \delta > 0$. Then, we have

$$e_n \leq \delta f_n, \quad (76)$$

where

$$f_n = \frac{\Gamma(n + \mu)}{n!} \sum_{k=0}^{n-1} \frac{k!}{\Gamma(k + 1 + \mu)}. \quad (77)$$

Moreover,

$$f_n \begin{cases} \leq \frac{1}{1 - \mu}, & 0 < \mu < 1, \\ \leq \ln n + 1, & \mu = 1, \\ \underset{n \rightarrow \infty}{\sim} \frac{1}{\Gamma(\mu + 1)} \frac{n^{\mu-1}}{\mu - 1}, & \mu > 1. \end{cases} \quad (78)$$

Proof. We proceed by mathematical induction. To begin, let us observe that $e_1 \leq \delta$ by the convention that $\sum_{i=1}^0 = 0$. Hence, $f_1 = 1$. Suppose that $e_i \leq \delta f_i$ for $1 \leq i \leq n - 1$. Due to this inductive assumption we have

$$e_n \leq \delta \left(\frac{\mu}{n} \sum_{i=1}^{n-1} f_i + 1 \right). \quad (79)$$

We claim that the sequence f_i defined in (77) satisfies the following difference equation

$$\frac{\mu}{n} \sum_{i=1}^{n-1} f_i + 1 = f_n, \quad (80)$$

which combined (79) proves the inductive assertion. When we subtract (80) written for $n + 1$ the equation for f_n we can obtain a local equation

$$(n + 1)f_{n+1} - (n + \mu)f_n - 1 = 0. \quad (81)$$

Switching back to f_n and rearranging we arrive at the recurrence

$$f_n = \left(1 + \frac{\mu - 1}{n}\right) f_n + \frac{1}{n}. \quad (82)$$

The above can be iterated to yield

$$f_n = \prod_{i=2}^n \left(1 + \frac{\mu - 1}{i}\right) + \sum_{i=0}^{n-2} \frac{1}{n-2} \prod_{j=1}^i \left(1 + \frac{\mu - 1}{n-j+1}\right). \quad (83)$$

Further, the products can be simplified considerably when we notice that

$$\prod_{i=2}^n \left(1 + \frac{\mu - 1}{i}\right) = \frac{(1 + \mu)(2 + \mu) \dots (n + \mu - 1)}{n!} = \frac{1}{n!} \frac{\Gamma(n + \mu)}{\Gamma(\mu + 1)}, \quad (84)$$

and similarly for the second one. Consequently, we arrive at

$$\begin{aligned} f_n &= \frac{\Gamma(n + \mu)}{n!} \left(\frac{1}{\Gamma(\mu + 1)} + \sum_{k=2}^n \frac{1}{k} \frac{k!}{\Gamma(k + \mu)} \right) = \frac{\Gamma(n + \mu)}{n!} \left(\frac{1}{\Gamma(\mu + 1)} + \sum_{k=1}^{n-1} \frac{k!}{\Gamma(k + 1 + \mu)} \right) \\ &= \frac{\Gamma(n + \mu)}{n!} \sum_{k=0}^{n-1} \frac{k!}{\Gamma(k + 1 + \mu)}, \end{aligned} \quad (85)$$

which is (77) and solves the recurrence.

In order to show (78) it suffices to consider the recurrence (80). Suppose that $0 < \mu < 1$, then $f_1 = 1 < 1/(1 - \mu)$. Further, if $f_i \leq 1/(\mu - 1)$ then

$$f_n \leq \frac{\mu}{n} \sum_{i=1}^{n-1} \frac{1}{1 - \mu} + 1 \leq \frac{\mu}{1 - \mu} + 1 = \frac{1}{1 - \mu}. \quad (86)$$

Next, for $\mu = 1$ we trivially have $f_1 = 1 = \ln 1 + 1$, and further by inductive assumption

$$f_n \leq \frac{1}{n} \sum_{i=1}^{n-1} (\ln i + 1) + 1 \leq \frac{1}{n} \int_1^n (\ln x + 1) dx + 1, \quad (87)$$

where we have used the fact that the sum is bounded by an appropriate integral. Evaluating, we obtain

$$f_n \leq \frac{1}{n} x \ln x \Big|_1^n + 1 = \ln n + 1. \quad (88)$$

Next, for the case $\mu > 1$ it is convenient to use the exact formula for f_n , that is (77). Then

$$f_n \sim n^{\mu-1} \sum_{k=0}^{\infty} \frac{k!}{\Gamma(k + 1 + \mu)} \quad \text{as } n \rightarrow \infty, \quad (89)$$

where we have used Stirling's formula for the prefactor and to ascertain the series convergence: $k!/\Gamma(k + 1 + \mu) \sim k^\mu$ as $k \rightarrow \infty$. We can find the exact form of the above sum by using the relation between beta and gamma functions

$$\sum_{k=0}^{\infty} \frac{k!}{\Gamma(k + 1 + \mu)} = \frac{1}{\Gamma(\mu)} \sum_{k=0}^{\infty} \frac{\Gamma(k + 1)\Gamma(\mu)}{\Gamma(k + 1 + \mu)} = \frac{1}{\Gamma(\mu)} \sum_{k=0}^{\infty} \int_0^1 (1 - x)^{\mu-1} x^k dx, \quad (90)$$

and by Tonelli's theorem we can exchange the order of summation and integration

$$\sum_{k=0}^{\infty} \frac{k!}{\Gamma(k+1+\mu)} = \frac{1}{\Gamma(\mu)} \int_0^1 (1-x)^{\mu-1} \sum_{k=0}^{\infty} x^k dx = \frac{1}{\Gamma(\mu)} \int_0^1 (1-x)^{\mu-2} dx = \frac{1}{(\mu-1)\Gamma(\mu)}, \quad (91)$$

which proves the last assertion. \square

For a thorough presentation of similar results see [1]. Next, we prove boundedness of the numerical approximation.

Lemma 2. *Let v_n be the numerical approximation of $v(z_n)$ calculated from (48). Fix sufficiently small number $\epsilon > 0$ and choose $h > 0$ small enough for $(z_n)^{-(m+1)(\gamma+1)/m} \sum_{i=0}^{n-1} |\delta_i(h)| < \epsilon$. Then, for $n \geq 1$ we have*

$$0 < \left(K_- \left(\beta \left(\gamma + 1, \frac{\gamma + 1}{m} + 1 \right) - \epsilon \right) \right)^{\frac{1}{m}} \leq v_n \leq \left(K_- \left(\beta \left(\gamma + 1, \frac{\gamma + 1}{m} + 1 \right) + \epsilon \right) \right)^{\frac{1}{m}}, \quad (92)$$

provided that the initial step v_0 satisfies the same inequality. Here, $\beta(\cdot, \cdot)$ denotes the beta function.

Proof. We will proceed by induction. The first step is satisfied by the assumption. Suppose further that v_i satisfies (92) for all $0 \leq i < n-1$. We will show that the same is true for v_n . To this end, write $V_-^{1/m} \leq v_i \leq V_+^{1/m}$ where V_{\pm} are defined in (92). By (48) and (35) we have

$$v_n^{m+1} \geq V_-^{\frac{1}{m}} K_- z_n^{-\frac{(m+1)(\gamma+1)}{m}} h \sum_{i=0}^{n-1} w_{n,i} (z_n - z_i)^{\gamma} z_i^{\frac{\gamma+1}{m}}. \quad (93)$$

Now, according to (47) we have

$$h \sum_{i=0}^{n-1} w_{n,i} (z_n - z_i)^{\gamma} z_i^{\frac{\gamma+1}{m}} = \int_0^{z_n} (z_n - s)^{\gamma} s^{\frac{\gamma+1}{m}} ds = z_n^{\frac{(\gamma+1)(m+1)}{m}} \beta \left(\gamma + 1, \frac{\gamma + 1}{m} + 1 \right) - \sum_{i=0}^{n-1} \delta_i(h). \quad (94)$$

Combining the two above expressions we obtain

$$v_n \geq V_-^{\frac{1}{m(m+1)}} \left(K_- \left(\beta \left(\gamma + 1, \frac{\gamma + 1}{m} + 1 \right) - z_n^{-\frac{(m+1)(\gamma+1)}{m}} \delta_n(h) \right) \right)^{\frac{1}{m+1}}. \quad (95)$$

Now, since by the assumption the remainder is smaller than ϵ we can write

$$v_n \geq V_-^{\frac{1}{m(m+1)}} \left(K_- \left(\beta \left(\gamma + 1, \frac{\gamma + 1}{m} + 1 \right) - \epsilon \right) \right)^{\frac{1}{m+1}} = V_-^{\frac{1}{m(m+1)}} V_-^{\frac{1}{m+1}} = V_-^{\frac{1}{m}}, \quad (96)$$

what completes the induction. The proof of the upper bound proceeds identically. \square

As it will be seen in the following main results, the boundedness from below play a crucial role in the proof.

A remark concerning the nature of the nonlinearity in (39) can be revealing. Note that if we substitute $f = y^{m+1}$ then the equation transforms into

$$f(z) = \int_0^z K(z, s) f(s)^{\frac{1}{m+1}} ds, \quad (97)$$

in which the nonlinearity is manifestly nonlipschitzian. Therefore, we cannot use the general theory to conclude the convergence. To wit, for the Lipschitz nonlinearity we are always able to reduce the analysis of the method's error e_n to investigations of the following recurrence inequality (see [45])

$$|e_n| \leq \mu h \sum_{i=1}^{n-1} |e_i| + \delta(h), \quad (98)$$

where μ and $\nu = \nu(h)$ are independent of n . Using the well-known discrete version of the Gronwall-Bellman's lemma (G-B) we can solve the above to yield (compare with our Lemma 1)

$$|e_n| \leq \delta(h)e^{\mu nh}. \quad (99)$$

The term $\delta(h)$ depends on the local consistency error and vanishes for $h \rightarrow 0$. Moreover, since we are comparing the numerical and exact solutions at a fixed point, we have $nh \rightarrow \text{const.}$. Therefore, $e_n \rightarrow 0$ and the method is convergent. The lipschitzian character of the nonlinearity makes the proof similar as in the linear equations. For the non-Lipschitz case we cannot in general write (98) and thus the arguments have to be different and more subtle. Notice that this difficulty is the very consequence of the degeneracy of the main equation (1). We summarize the result in the following theorem.

Theorem 2. *Fix $z \in (0, 1]$ and chose the weights of the quadrature (47) according to (62) and (65) while the starting values from (72) and (74). Then, if*

$$\mu_m := \frac{4K_+}{(m+1)V_-} < 3, \quad (100)$$

the scheme (48) is convergent to the nontrivial solution of (43) with an order at least equal to

$$\min\{2, 3 - \mu_m\}. \quad (101)$$

Here, $V_-^{1/m}$ is the lower bound for both $v = v(z)$ and v_n .

Proof. Let us define the error of the numerical approximation by $e_n = v(z_n) - v_n$, where $v(z)$ is the solution of (43) while v_n comes from (48). Now, the difference between these two equations is

$$v(z_n)^{m+1} - v_n^{m+1} = z_n^{-\frac{(m+1)(\gamma+1)}{m}} \left(\int_0^z K(z, s) s^{\frac{\gamma+1}{m}} v(s) ds - \sum_{i=0}^{n-1} w_{n,i}(h) v_i \right). \quad (102)$$

With the use of (47) and the construction leading to (66) we further obtain

$$v(z_n)^{m+1} - v_n^{m+1} = z_n^{-\frac{(m+1)(\gamma+1)}{m}} \sum_{i=1}^{n-1} w_{n,i}(h) e_i + \delta_n(h), \quad (103)$$

where the remainder $\delta_n(h)$ satisfies (67) and the zero term vanishes due to exact starting value (72). On the other hand, by the mean value theorem we can write

$$v(z_n)^{m+1} - v_n^{m+1} = (m+1)\xi_n^m e_n, \quad (104)$$

where ξ_n lies between $v(z_n)$ and v_n . Next, by combining the two above equations we have

$$(m+1)\xi_n^m |e_n| \leq z_n^{-\frac{(m+1)(\gamma+1)}{m}} \sum_{i=1}^{n-1} |w_{n,i}(h)| |e_i| + Ch^2, \quad (105)$$

where C is a constant explicitly defined in (67). The boundedness of both $v(z_n)$ and v_n (see (44) and Lemma 2)) implies that $\xi_n \geq V_-$ for some constant and thus

$$|e_n| \leq \frac{z_n^{-\frac{(m+1)(\gamma+1)}{m}}}{(m+1)V_-} \sum_{i=1}^{n-1} |w_{n,i}(h)| |e_i| + \frac{Ch^2}{(m+1)V_-}, \quad (106)$$

which is a recurrence inequality which will eventually be solved with invoking Grönwall-Bellman's lemma. To see this observe that by (62) and (65) we have for example

$$|w_{n,i}(h)| \leq \frac{4K_+}{n} z_n^{\frac{(m+1)(\gamma+1)}{m}}, \quad (107)$$

where the factor $4/n$ comes from the fact that $|s - z_i| \leq 2h$ on each subinterval of length $2/n$, K_+ is the bound on the kernel (35), and the integrand is not larger than 1. This leads to

$$|e_n| \leq \frac{4K_+}{(m+1)V_-} \frac{1}{n} \sum_{i=1}^{n-1} |e_i| + \frac{Ch^2}{(m+1)V_-} =: \frac{\mu_m}{n} \sum_{i=1}^{n-1} |e_i| + \delta. \quad (108)$$

Invoking Lemma 1 thus yields

$$|e_n| \leq \frac{Ch^2}{(m+1)V_-} f_n, \quad (109)$$

where f_n is defined in (77). Now, if $0 < \mu_m < 1$, the error $|e_n|$ is bounded for all n , i.e.

$$|e_n| \leq \frac{Ch^2}{(m+1)V_- - 4K_+} \quad (110)$$

Further, for $\mu_m > 1$ we have

$$|e_n| \leq \frac{Ch^2}{(m+1)V_-} f_n \sim \frac{Ch^2}{(\mu_m - 1)\Gamma(\mu_m)(m+1)V_-} n^{\mu_m-1} \sim \frac{Cz^{\mu_m-1}}{(\mu_m - 1)\Gamma(\mu_m)(m+1)V_-} h^{3-\mu_m}, \quad (111)$$

as $n \rightarrow \infty$. Here, we have used the fact that $nh \rightarrow z$. Similarly, the marginal case $\mu = 1$ yields a convergence of order $-h^2 \ln h$. The proof is complete. \square

According to (101) the method retains its order for sufficiently small μ_m . More specifically, when $\mu_m < 1$ the method is second order accurate. This estimate gradually becomes worse until $\mu_m = 3$ when the theorem does not guarantee convergence. Note, however, that choosing sufficiently large m we always can obtain a second order method. The fact that, according to the theorem, the order of the method can be smaller than the order of the quadrature is probably the consequence of severe nonlinearity of the equation. This, in turn, corresponds to the degeneracy of the original PDE (1) what throughout the years has proved to lay significant difficulties for both theoretical and numerical studies (see for ex. [25, 33]). The main difference between the classical case of Lipschitzian nonlinearity is the occurrence of $1/n$ instead of h in the nonlocal recurrence (108). This forces us to use Lemma 1) rather than the classical discrete Grönwall-Bellman's lemma. Since $1/n$ changes in each recurrence step the assertion is somewhat different yielding a loss in convergence order. However, for $0 < \mu_m < 1$ the error is $O(h^2)$ as $h \rightarrow 0^+$ for any $n > 0$. A very thorough account of numerical methods for integral equations with Lipschitzian nonlinearities can be found in [45].

4 Numerical examples

In this section we present several numerical examples. We start with a simple integral equation that can be solved exactly in a closed form. Next, we consider a more complex equation and use it to verify the order of convergence. Finally, we proceed to solving the time-fractional diffusion problems summarized in Tab. 1. Numerical calculations have been conducted in Julia programming language. Integrals appearing in weights (62) and (65) have been calculated with the QuadGK package that utilizes Gauss-Kronrod adaptive quadrature.

| | $\gamma = 0$ | $\gamma = 0.5$ | $\gamma = \sqrt{2}$ | $\gamma = \pi$ |
|-----------|------------------------|------------------------|------------------------|------------------------|
| $m = 1$ | 1.11×10^{-16} | 2.90×10^{-11} | 8.94×10^{-13} | 2.20×10^{-14} |
| $m = 2$ | 2.40×10^{-10} | 1.18×10^{-10} | 1.19×10^{-11} | 1.60×10^{-13} |
| $m = 10$ | 1.90×10^{-10} | 1.01×10^{-10} | 4.26×10^{-11} | 4.71×10^{-11} |
| $m = 100$ | 1.85×10^{-11} | 2.03×10^{-11} | 1.97×10^{-11} | 1.01×10^{-11} |

Table 2: Maximal absolute error for a numerical approximation of the solution of (43) with $K(z, s) = (z - s)^\gamma$ for various γ and m . The number of interval divisions is $N = 10$.

| m | 1 | 5 | 10 | 15 | 20 | 50 | 100 |
|-------|------|------|------|------|------|------|------|
| order | 2.02 | 2.00 | 1.96 | 1.92 | 1.90 | 1.86 | 1.84 |

Table 3: Numerically calculated order of convergence of the numerical methods based on rectangular approximation (58) and trapezoidal (62), (65). The base for Aitken's estimation is $N = 100$.

4.1 Exact constant solution

We start with a simple illustration of the exactness of our numerical methods. Let $K(z, s) = (z - s)^\gamma$ in (43). According to (45) the integral equation has then a constant solution (that is, a power function is a solution of (39)). In Tab. 2 we have collected the maximal absolute error (first norm) of the numerical approximation (48) with second order weights (62) and (65). Note that in calculations we have used $N = 10$ which is relatively small. Our experiments showed that increasing the number of interval divisions does not improve the error. Notice also that the smallest error $O(10^{-16})$ appears for the case $\gamma = 0$ and $m = 1$ for which the exact solution is equal to $1/2$. We expect that since that number is exactly representable in computer arithmetic system since this is the order of used machine epsilon. The majority of simulations concluded that the error is of order of $O(10^{-11})$ we can conclude that the method performs very well and reproduces the exact solution with good accuracy.

4.2 Order of convergence

We will calculate the empirical order of convergence of our second order method and compare it with the rectangle scheme (58). This illustration will be completed with the use of the integral equation (43) with

$$K(z, s) = \frac{\sqrt{z - s}}{1 + \sin^2 s}. \quad (112)$$

Obviously, the kernel satisfies our assumptions on the boundedness (35) with $K_- = 1/2$ and $K_+ = 1$. The order of convergence is estimated with the extrapolation technique known as Aitken's method (see [45])

$$\text{order} \approx \log_2 \frac{|v_N^{(2N)} - v_N^{(N)}|}{|v_N^{(4N)} - v_N^{(2N)}|}, \quad (113)$$

which compares the numerical solution evaluated at $z = 1$ (the worst case) with calculations for N , $2N$, and $4N$ steps. The summary of obtained results is presented in Tab. 3. We can see that the estimated order is near 2 however, for larger m it is somewhat lower. This fact probably originates in the necessity of taking a very high order root in the equation. Moreover, for this example, we have $\mu_m = 0.8 < 3$ what satisfies the assumption of Theorem 2. We can thus see that, as anticipated, the method is of second order. Moreover, similar calculations have been done for the rectangle method (58) and the results were more uniform: the estimated order was equal to 0.99 for all considered m .

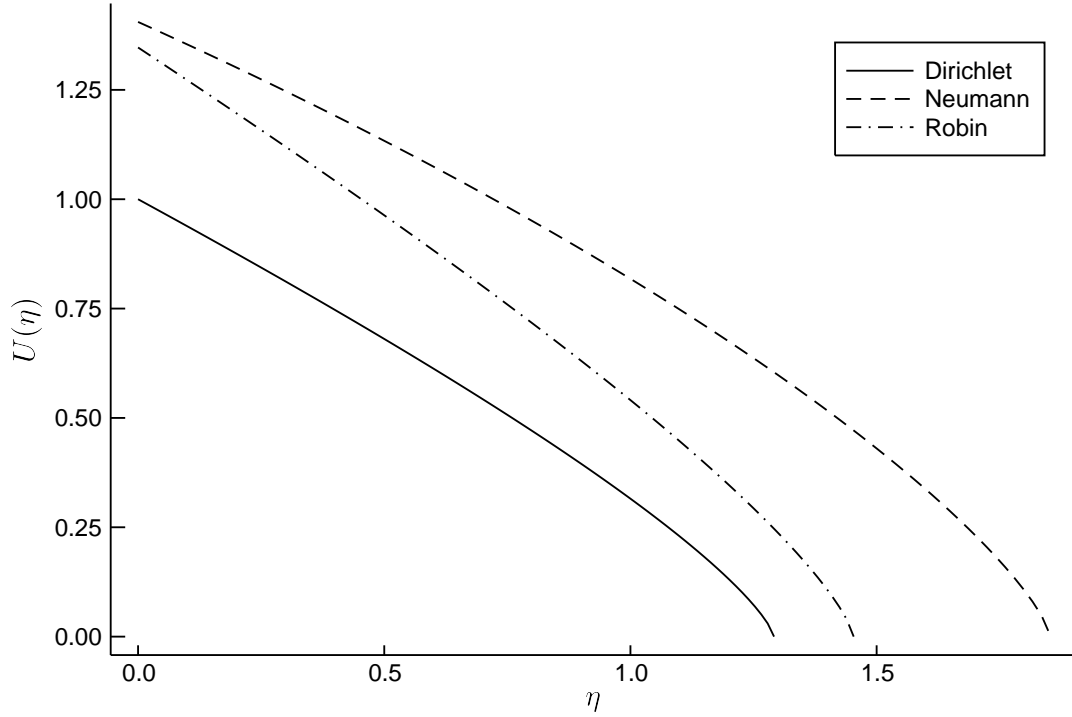


Figure 1: Exemplary self-similar solutions of the time-fractional porous medium equation (1). Here, $\alpha = 0.5$ and $m = 2$.

4.3 Anomalous diffusion

Now, we proceed to the subject of the main interest - the time-fractional porous medium equation. We use the kernel (28) which conveniently can be written with the help of incomplete beta functions

$$K(z, u) = \frac{m+1}{\Gamma(1-\alpha)} [B(1-u)\beta(1-\alpha, a+b+1, 1-w) + (A+B)((1-u)\beta(1-\alpha, a+b+1, 1-w) - (1-z)\beta(1-\alpha, a+1, 1-w))], \quad (114)$$

where

$$\beta(a, b, z) = \int_0^z t^{a-1}(1-t)^{b-1}dt, \quad (115)$$

and A, B, a, b are chosen according to the boundary conditions summarized in Tab. 1. Some exemplary plots of the self-similar solutions of (1) are presented on Fig. 1.

First, we estimate the minimal value of parameter m , say m_0 , for which the assumption of the Theorem 2 is satisfied for the most important - Dirichlet - boundary condition. According to (100) it is equal to a zero of a function $m \mapsto \mu_m - 3$. In order to estimate that we have to find K_+ which can be a-priori calculated from (32). However, a more accurate bound comes from the estimate

$$K_+ \geq \sup_{0 \leq u \leq z \leq 1} \frac{K(z, u)}{(z-u)^{1-\alpha}}, \quad (116)$$

which can be found numerically. Note also that when we compare the formulas (32) and (92) we can expect that the ratio K_+/V_- is constant with respect to m . Whence μ_m should be $O(m^{-1})$ as $m \rightarrow \infty$. Results of numerical estimation are presented in Tab. 4. We can see that usually the value of m_0 is slightly larger than 1 and closes to 3 for very small α . In applications, one usually finds $m \approx 7-8$ with $\alpha \in [0.6, 1]$ [62] and, for these important cases, we know that Theorem 2 guarantees convergence.

| α | 0.99 | 0.9 | 0.8 | 0.7 | 0.6 | 0.5 | 0.4 | 0.3 | 0.2 | 0.1 | 0.01 |
|----------|------|------|------|------|------|------|------|------|------|------|------|
| m_0 | 1.10 | 1.14 | 1.19 | 1.25 | 1.28 | 1.35 | 1.66 | 1.98 | 2.31 | 2.62 | 2.84 |

Table 4: Estimated critical values of m for which the assumptions of Theorem 2 are satisfied for the case of anomalous diffusion.

| $m \backslash \alpha$ | 0.01 | 0.1 | 0.3 | 0.5 | 0.7 | 0.9 | 0.99 |
|-----------------------|------|------|------|------|------|------|------|
| 1 | 1.84 | 1.98 | 2.01 | 2.00 | 2.09 | 2.10 | 2.13 |
| 3 | 1.80 | 1.98 | 1.99 | 1.98 | 1.97 | 1.96 | 1.96 |
| 5 | 1.74 | 1.92 | 1.92 | 1.92 | 1.91 | 1.89 | 1.89 |
| 7 | 1.71 | 1.88 | 1.88 | 1.87 | 1.87 | 1.91 | 1.86 |
| 10 | 1.70 | 1.85 | 1.85 | 1.84 | 1.84 | 1.86 | 1.83 |
| 20 | 1.73 | 1.85 | 1.84 | 1.83 | 1.83 | 1.85 | 1.82 |

Table 5: Order of convergence for the trapezoidal method applied to subdiffusion for different α and m .

Similarly as above we can estimate the order of convergence of the trapezoid method. We again use Aitken's algorithm and present the results in Tab. 5. As can be seen the estimated order stays near 2 especially for moderate values of m what has also been observed in the previous example.

As a further verification of our method we can compute the wetting front position η^* for the classical case $\alpha = 1$ and compare it with results from [47]. In that work, the values of η^* were computed with a use of power series and we can treat them as exact (up to 9 decimal places). Our calculations for $m = 2$ are summarized in Tab. 6. Results for other values of m are very similar. Notice that even for a very small number of subdivisions we obtain an error of order $O(10^{-5})$ which is a consequence of the second order accuracy.

Wetting fronts for subdiffusive case cannot easily be compared with exact values. However, we have some useful asymptotics. First, let us consider the Dirichlet boundary condition for which we know that (see [55])

$$\eta^* = O(m^{-1/2}) \quad m \rightarrow \infty. \quad (117)$$

This relation can also be obtained by combining the value for η^* taken from Tab. 1 with estimates (36) and noting that $K_+ \propto m + 1$. Our numerical simulations are depicted on Fig. 2. Notice that the above asymptotic behaviour is evident even for small values of m , i.e. in a log-log scale all lines become parallel to $m^{-1/2}$.

A similar reasoning can be applied to Neumann and Robin conditions. To this end we need an asymptotic behaviour of the derivative $y'(1)$ for $m \rightarrow \infty$. First, notice that due to (32) and (36) we have $\|y\| = O((1 + m)^{1/m}) = O(1)$ for large m . Then, from (25) we obtain

$$\|y'\| = O\left(\frac{1}{m+1}\right) \quad \text{as } m \rightarrow \infty, \quad (118)$$

| N | 10 | 20 | 50 | 100 | 200 | 500 | 1500 |
|-----------------------------|----------------------|----------------------|----------------------|----------------------|----------------------|----------------------|----------------------|
| $ \eta^* - \eta_{exact}^* $ | 1.1×10^{-4} | 2.9×10^{-5} | 4.6×10^{-6} | 1.1×10^{-6} | 2.8×10^{-7} | 4.5×10^{-8} | 5.4×10^{-9} |

Table 6: The error in calculating wetting front position for $\alpha = 1$ and $m = 2$. The exact value has been taken from [49].

uniformly for $\alpha \in (0, 1)$. Next, using the value from Tab. 1 we can write

$$\eta^* = \left(\frac{1}{y^m(1)y'(1)} \right)^{\frac{m}{m+2}} = O\left(\frac{m+1}{m+1} \right)^{\frac{m}{m+2}} = O(1) \quad m \rightarrow \infty. \quad (119)$$

for Neumann condition. Similarly, the wetting front for the Robin case also is bounded for large m . We can see on Fig. 2 that this observation is confirmed with numerical simulations, that is for large m wetting fronts converge to fixed values.

5 Conclusion

We have constructed a convergent second order method for solving (39) which can encompass self-similar solutions of a time-fractional porous medium equation on the half-line. This fact is a consequence of a series of transformations that changed a nonlocal nonlinear PDE into an ordinary Volterra integral equation. The interesting feature of the latter is a non-Lipschitz nonlinearity that possess some difficulties in numerical analysis.

Our second order method is based on a linear (trapezoidal) reconstruction has been applied to several examples. Numerical calculations confirmed convergence with desired accuracy. We have observed that it suffices to use a relatively small number of interval subdivisions in order to obtain a decent approximation of the exact solution. Moreover, the method reproduced the asymptotic behaviour of the wetting front for large values of m in three considered boundary conditions. All calculations have been conducted on a personal computer with a four core Intel® i5-1035G4 processor. Each simulation took at most few tens of seconds. This can be compared with our previous observation made in [55] stating that our numerical method is orders of magnitude faster than the implicit finite difference scheme applied to (1). The nonlocality, nonlinearity, stiffness, and degeneracy of the governing equation require much computing power to resolve. Transforming the original PDE into an ordinary Volterra equation reduces one degree of freedom and simplifies the free-boundary problem which facilitates the method's construction and performance. Therefore, our trapezoidal method is an accurate and fast way of computing self-similar solutions of the time-fractional porous medium equation on the half-line.

Acknowledgement

L.P. has been supported by the National Science Centre, Poland (NCN) under the grant Sonata Bis with a number NCN 2020/38/E/ST1/00153.

References

- [1] William F Ames and BG Pachpatte. *Inequalities for differential and integral equations*, volume 197. Academic press, 1997.
- [2] Todd Arbogast and Mary F Wheeler. A nonlinear mixed finite element method for a degenerate parabolic equation arising in flow in porous media. *SIAM Journal on Numerical Analysis*, 33(4):1669–1687, 1996.
- [3] MR Arias, R Benítez, and VJ Bolós. Non-lipschitz homogeneous volterra integral equations. In *Modern Mathematics and Mechanics*, pages 237–259. Springer, 2019.
- [4] FV Atkinson and LA Peletier. Similarity profiles of flows through porous media. *Archive for Rational Mechanics and Analysis*, 42(5):369–379, 1971.
- [5] Christopher TH Baker. A perspective on the numerical treatment of volterra equations. *Journal of computational and applied mathematics*, 125(1-2):217–249, 2000.

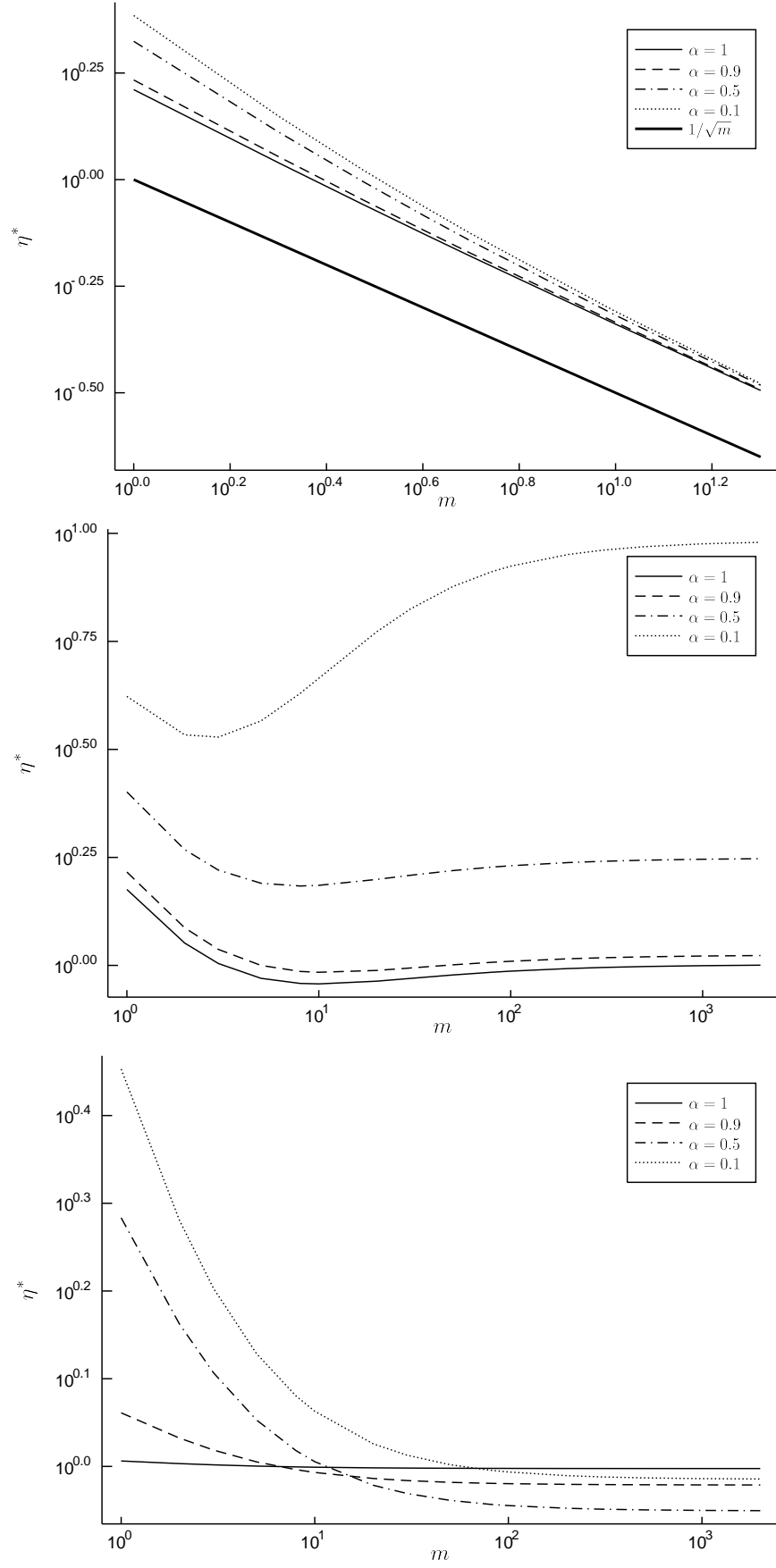


Figure 2: Wetting front position η^* with respect to m for a Dirichlet (top), Neumann (middle), and Robin (bottom) boundary conditions shown in a double logarithmic scale.

- [6] Dumitru Baleanu, Kai Diethelm, Enrico Scalas, and Juan J Trujillo. *Fractional calculus: models and numerical methods*, volume 3. World Scientific, 2012.
- [7] AH Bhrawy. A Jacobi spectral collocation method for solving multi-dimensional nonlinear fractional sub-diffusion equations. *Numerical Algorithms*, 73(1):91–113, 2016.
- [8] Piotr Biler, Cyril Imbert, and Grzegorz Karch. The nonlocal porous medium equation: Barenblatt profiles and other weak solutions. *Archive for Rational Mechanics and Analysis*, 215(2):497–529, 2015.
- [9] Matteo Bonforte, Alessio Figalli, and Juan Luis Vázquez. Sharp global estimates for local and nonlocal porous medium-type equations in bounded domains. *Analysis & PDE*, 11(4):945–982, 2018.
- [10] Hermann Brunner. *Volterra Integral Equations: An Introduction to Theory and Applications*, volume 30. Cambridge University Press, 2017.
- [11] Evelyn Buckwar. *Iterative Approximation of the Positive Solutions of a Class of Nonlinear Volterra-type Integral Equations*. Logos Verlag, 1997.
- [12] Evelyn Buckwar. On a nonlinear Volterra integral equation. In *Volterra equations and applications*, pages 157–162. CRC Press, 2000.
- [13] Evelyn Buckwar. Existence and uniqueness of solutions of abel integral equations with power-law nonlinearities. *Nonlinear Analysis: Theory, Methods & Applications*, 63(1):88–96, 2005.
- [14] PJ Bushell. On a class of Volterra and Fredholm non-linear integral equations. In *Mathematical Proceedings of the Cambridge Philosophical Society*, volume 79(2), pages 329–335. Cambridge Univ Press, 1976.
- [15] PJ Bushell. The cayley-hilbert metric and positive operators. *Linear Algebra and its Applications*, 84:271–280, 1986.
- [16] PJ Bushell and W Okrasinski. Nonlinear volterra integral equations with convolution kernel. *Journal of the London Mathematical Society*, 2(3):503–510, 1990.
- [17] Luis Caffarelli and Luis Silvestre. An extension problem related to the fractional laplacian. *Communications in Partial Differential Equations*, 32(8):1245–1260, 2007.
- [18] Luis A Caffarelli and Juan L Vazquez. Nonlinear porous medium flow with fractional potential pressure. *arXiv preprint arXiv:1001.0410*, 2010.
- [19] Nicole Cusimano, Félix del Teso, Luca Gerardo-Giorda, and Gianni Pagnini. Discretizations of the spectral fractional laplacian on general domains with Dirichlet, Neumann, and Robin boundary conditions. *SIAM Journal on Numerical Analysis*, 56(3):1243–1272, 2018.
- [20] Arturo de Pablo, Fernando Quiros, Ana Rodriguez, and Juan Luis Vazquez. A fractional porous medium equation. *Advances in Mathematics*, 226(2):1378–1409, 2011.
- [21] Diego del Castillo-Negrete, BA Carreras, and VE Lynch. Nondiffusive transport in plasma turbulence: a fractional diffusion approach. *Physical Review Letters*, 94(6):065003, 2005.
- [22] Félix del Teso. Finite difference method for a fractional porous medium equation. *Calcolo*, 51(4):615–638, 2014.
- [23] Félix del Teso, Jørgen Endal, and Espen R Jakobsen. Robust numerical methods for local and nonlocal equations of porous medium type. part i: Theory. *arXiv preprint arXiv:1801.07148*, 2018.
- [24] Felix del Teso, Jørgen Endal, and Espen R Jakobsen. Robust numerical methods for nonlocal (and local) equations of porous medium type. part ii: Schemes and experiments. *SIAM Journal on Numerical Analysis*, 56(6):3611–3647, 2018.

- [25] Emmanuele DiBenedetto and David Hoff. An interface tracking algorithm for the porous medium equation. *Transactions of the American Mathematical Society*, 284(2):463–500, 1984.
- [26] Kai Diethelm and Neville J Ford. Analysis of fractional differential equations. *Journal of Mathematical Analysis and Applications*, 265(2):229–248, 2002.
- [27] Jean-Daniel Djida, Juan J Nieto, and Iván Area. Nonlocal time-porous medium equation: weak solutions and finite speed of propagation. *Discrete Continuous Dyn. Syst. Ser. B*, 2018.
- [28] Jean-Daniel Djida, Juan J Nieto, and Iván Area. Nonlocal time porous medium equation with fractional time derivative. *Revista Matemática Complutense*, 32(2):273–304, 2019.
- [29] Carsten Ebmeyer. Error estimates for a class of degenerate parabolic equations. *SIAM Journal on Numerical Analysis*, 35(3):1095–1112, 1998.
- [30] Monika Eisenmann and Eskil Hansen. Convergence analysis of domain decomposition based time integrators for degenerate parabolic equations. *Numerische mathematik*, 140(4):913–938, 2018.
- [31] A El Abd, SE Ki?hanov, M Taman, ?? Nazarov, DP Kozlenko, and Wael M Badawy. Determination of moisture distributions in porous building bricks by neutron radiography. *Applied Radiation and Isotopes*, page 108970, 2019.
- [32] Abd El-Ghany El Abd and Jacek J Milczarek. Neutron radiography study of water absorption in porous building materials: anomalous diffusion analysis. *Journal of Physics D: Applied Physics*, 37(16):2305, 2004.
- [33] Emmrich Etienne and David Šiška. Full discretization of the porous medium/fast diffusion equation based on its very weak formulation. *Communications in Mathematical Sciences*, 10(4):1055–1080, 2012.
- [34] Kurt Frischmuth, Neville J Ford, and John T Edwards. Volterra integral equations with non-lipschitz nonlinearity. In *Rostocker Mathematisches Kolloquium*, volume 51, pages 65–82, 1997.
- [35] Francisco J Gaspar and Carmen Rodrigo. Multigrid waveform relaxation for the time-fractional heat equation. *SIAM Journal on Scientific Computing*, 39(4):A1201–A1224, 2017.
- [36] Gustaf Gripenberg. Unique solutions of some Volterra integral equations. *Mathematica Scandinavica*, 48(1):59–67, 1981.
- [37] AK Head. Dislocation group dynamics iii. similarity solutions of the continuum approximation. *Philosophical Magazine*, 26(1):65–72, 1972.
- [38] Yanghong Huang and Adam Oberman. Numerical methods for the fractional laplacian: A finite difference-quadrature approach. *SIAM Journal on Numerical Analysis*, 52(6):3056–3084, 2014.
- [39] Willi Jäger and Jozef Kačur. Solution of porous medium type systems by linear approximation schemes. *Numerische Mathematik*, 60(1):407–427, 1991.
- [40] Virginia S Kiryakova. *Generalized fractional calculus and applications*. CRC Press, 1993.
- [41] Joseph Klafter, SC Lim, and Ralf Metzler. *Fractional dynamics: recent advances*. World Scientific, 2012.
- [42] Rainer Klages, Günter Radons, and Igor M Sokolov. *Anomalous transport: foundations and applications*. John Wiley & Sons, 2008.
- [43] M Levandowsky, BS White, and FL Schuster. Random movements of soil amebas. *Acta Protozoologica*, 36:237–248, 1997.
- [44] Xianjuan Li and Chuanju Xu. A space-time spectral method for the time fractional diffusion equation. *SIAM Journal on Numerical Analysis*, 47(3):2108–2131, 2009.

- [45] Peter Linz. *Analytical and numerical methods for Volterra equations*, volume 7. SIAM, 1985.
- [46] Ralf Metzler and Joseph Klafter. The random walk’s guide to anomalous diffusion: a fractional dynamics approach. *Physics reports*, 339(1):1–77, 2000.
- [47] W Okrański. On approximate solutions to some nonlinear diffusion problems. *Zeitschrift für angewandte Mathematik und Physik ZAMP*, 44(4):722–731, 1993.
- [48] W Okrasinski. On nontrivial solutions to some nonlinear ordinary differential equations. *Journal of mathematical analysis and applications*, 190(2):578–583, 1995.
- [49] W Okrański and S Vila. Power series solutions to some nonlinear diffusion problems. *Zeitschrift für angewandte Mathematik und Physik ZAMP*, 44(6):988–997, 1993.
- [50] Yakov Pachepsky, Dennis Timlin, and Walter Rawls. Generalized richards’ equation to simulate water transport in unsaturated soils. *Journal of Hydrology*, 272(1):3–13, 2003.
- [51] Łukasz Płociniczak. Approximation of the Erdélyi–Kober operator with application to the time-fractional porous medium equation. *SIAM Journal on Applied Mathematics*, 74(4):1219–1237, 2014.
- [52] Łukasz Płociniczak. Analytical studies of a time-fractional porous medium equation. derivation, approximation and applications. *Communications in Nonlinear Science and Numerical Simulation*, 24(1):169–183, 2015.
- [53] Łukasz Płociniczak. Diffusivity identification in a nonlinear time-fractional diffusion equation. *Fractional Calculus and Applied Analysis*, 19:883–866, 2016.
- [54] Łukasz Płociniczak. Derivation of the nonlocal pressure form of the fractional porous medium equation in the hydrological setting. *Communications in Nonlinear Science and Numerical Simulation*, 76:66–70, 2019.
- [55] Łukasz Płociniczak. Numerical method for the time-fractional porous medium equation. *SIAM Journal on Numerical Analysis*, 57(2):638–656, 2019.
- [56] Łukasz Płociniczak and Hanna Okrańska-Płociniczak. Numerical method for Volterra equation with a power-type nonlinearity. *Applied Mathematics and Computation*, 337:452–460, 2018.
- [57] Łukasz Płociniczak and Mateusz Świtała. Existence and uniqueness results for a time-fractional nonlinear diffusion equation. *Journal of Mathematical Analysis and Applications*, 462(2):1425–1434, 2018.
- [58] Igor Podlubny. *Fractional differential equations: an introduction to fractional derivatives, fractional differential equations, to methods of their solution and some of their applications*, volume 198. Academic press, 1998.
- [59] Iuliu Sorin Pop and Wen-An Yong. A numerical approach to degenerate parabolic equations. *Numerische Mathematik*, 92(2):357–381, 2002.
- [60] Stefan Schaufler, WP Schleich, and VP Yakovlev. Scaling and asymptotic laws in subrecoil laser cooling. *EPL (Europhysics Letters)*, 39(4):383, 1997.
- [61] Diana Stan, Félix del Teso, and Juan Luis Vázquez. Finite and infinite speed of propagation for porous medium equations with fractional pressure. *Comptes Rendus Mathématique*, 352(2):123–128, 2014.
- [62] HongGuang Sun, Mark M Meerschaert, Yong Zhang, Jianting Zhu, and Wen Chen. A fractal richards’ equation to capture the non-boltzmann scaling of water transport in unsaturated media. *Advances in Water Resources*, 52:292–295, 2013.
- [63] Titiwat Sungkaworn, Marie-Lise Jobin, Krzysztof Burnecki, Aleksander Weron, Martin J Lohse, and Davide Calebiro. Single-molecule imaging reveals receptor–g protein interactions at cell surface hot spots. *Nature*, 550(7677):543, 2017.

- [64] Charles Tadjeran, Mark M Meerschaert, and Hans-Peter Scheffler. A second-order accurate numerical approximation for the fractional diffusion equation. *Journal of Computational Physics*, 213(1):205–213, 2006.
- [65] Juan Luis Vázquez. *The porous medium equation: mathematical theory*. Oxford University Press, 2007.
- [66] Juan Luis Vázquez. Nonlinear diffusion with fractional laplacian operators. In *Nonlinear partial differential equations*, pages 271–298. Springer, 2012.
- [67] Juan Luis Vázquez. The mathematical theories of diffusion: Nonlinear and fractional diffusion. In *Non-local and Nonlinear Diffusions and Interactions: New Methods and Directions*, pages 205–278. Springer, 2017.
- [68] Santos B Yuste and Luis Acedo. An explicit finite difference method and a new von Neumann-type stability analysis for fractional diffusion equations. *SIAM Journal on Numerical Analysis*, 42(5):1862–1874, 2005.
- [69] Fanhai Zeng, Fawang Liu, Changpin Li, Kevin Burrage, Ian Turner, and Vo Anh. A Crank–Nicolson adi spectral method for a two-dimensional riesz space fractional nonlinear reaction-diffusion equation. *SIAM Journal on Numerical Analysis*, 52(6):2599–2622, 2014.